



Since January 2020 Elsevier has created a COVID-19 resource centre with free information in English and Mandarin on the novel coronavirus COVID-19. The COVID-19 resource centre is hosted on Elsevier Connect, the company's public news and information website.

Elsevier hereby grants permission to make all its COVID-19-related research that is available on the COVID-19 resource centre - including this research content - immediately available in PubMed Central and other publicly funded repositories, such as the WHO COVID database with rights for unrestricted research re-use and analyses in any form or by any means with acknowledgement of the original source. These permissions are granted for free by Elsevier for as long as the COVID-19 resource centre remains active.



Nanozyme-strip for rapid and ultrasensitive nucleic acid detection of SARS-CoV-2

Xiangqin Meng^{a,1}, Sijia Zou^{a,b,1}, Dandan Li^c, Jiuyang He^a, Ling Fang^d, Haojue Wang^d, Xiyun Yan^{a,e,f,**}, Demin Duan^{a,***}, Lizeng Gao^{a,e,*}

^a CAS Engineering Laboratory for Nanozyme, Institute of Biophysics, Chinese Academic of Science, Beijing, 100101, China

^b School of Basic Medical Science, Southwest Medical University, Luzhou, 646000, China

^c School of Medicine, Institute of Translational Medicine, Yangzhou University, Yangzhou, 225001, China

^d Xishan People's Hospital of Wuxi City, Wuxi, Jiangsu, 214105, China

^e Nanozyme Medical Center, School of Basic Medical Sciences, Zhengzhou University, Zhengzhou, 450052, China

^f Shenzhen Institute of Synthetic Biology, Shenzhen Institute of Advanced Technology, Chinese Academy of Sciences, Shenzhen, 518055, China

ARTICLE INFO

Keywords:

Nanozyme strips
Nucleic acid detection
SARS-CoV-2
Point-of-care testing
Recombinase polymerase amplification
HPV-16

ABSTRACT

The coronavirus disease 2019 (COVID-19) pandemic has created a huge demand for sensitive and rapid detection of severe acute respiratory syndrome coronavirus 2 (SARS-CoV-2). The current gold standard for SARS-CoV-2 detection is reverse transcription-polymerase chain reaction (RT-PCR)-based nucleic acid amplification. However, RT-PCR is time consuming and requires specialists and large instruments that are unattainable for point-of-care testing (POCT). To develop POCT for SARS-CoV-2, we combined recombinase polymerase amplification (RPA) and FeS₂ nanozyme strips to achieve facile nucleic acid amplification and subsequent colorimetric signal enhancement based on the high peroxidase-like activity of the FeS₂ nanozymes. This method showed a nucleic acid limit of detection (LOD) for SARS-CoV-2 of 200 copies/mL, close to that of RT-PCR. The unique catalytic properties of the FeS₂ nanozymes enabled the nanozyme-strip to amplify colorimetric signals via the nontoxic 3,3',5,5'-tetramethylbenzidine (TMB) substrate. Importantly, the detection of clinical samples of human papilloma virus type 16 (HPV-16) showed 100% agreement with previous RT-PCR results, highlighting the versatility and reliability of this method. Our findings suggest that nanozyme-based nucleic acid detection has great potential in the development of POCT diagnosis for COVID-19 and other viral infections.

1. Introduction

Coronavirus disease 2019 (COVID-19), which is caused by severe acute respiratory syndrome coronavirus 2 (SARS-CoV-2), was declared a global pandemic on March 11, 2020 by the World Health Organization, and has had a dramatic impact on life, health, society, and the economy (Wang et al., 2020). Although current vaccination rates is relatively high, SARS-CoV-2 variants, especially Omicron variants, can escape the

protection of the developed antibodies (Iketani et al., 2022; Li et al., 2020). In addition, effective drugs remain insufficient, particularly for severely ill patients. Therefore, timely large-scale screening to identify and quarantine positive patients continues to play a substantial role in the fight against the pandemic. At present, reverse transcription-polymerase chain reaction (RT-PCR) is the gold standard for SARS-CoV-2 detection due to its higher sensitivity and specificity than antigen and antibody tests (Shih et al., 2020). However, the lengthy

Abbreviations: AEC, 3-amino-9-ethylcarbazole; BSA, Bovine serum albumin; COVID-19, Coronavirus disease 2019; DAB, 3,3'-diaminobenzidine; EDS, Energy dispersive X-ray spectroscopy; HPV-16, Human papilloma virus type 16; LOD, Limit of detection; MERS-CoV, Middle East respiratory syndrome coronavirus; POCT, Point-of-care testing; PVC, Polyvinylchloride; PVP, Polyvinyl pyrrolidone; RPA, Recombinase polymerase amplification; RT-PCR, Reverse transcription-polymerase chain reaction; SAED, Selected area electron diffraction; SARS-CoV-2, Severe acute respiratory syndrome coronavirus 2; SEM, Scanning electron microscopy; TEM, Transmission electron microscopy; TMB, 3,3',5,5'-tetramethylbenzidine; XPS, X-ray photoelectron spectroscopy; XRD, X-ray diffraction.

* Corresponding author. CAS Engineering Laboratory for Nanozyme, Institute of Biophysics, Chinese Academic of Science, Beijing, 100101, China.

** Corresponding author. CAS Engineering Laboratory for Nanozyme, Institute of Biophysics, Chinese Academic of Science, Beijing, 100101, China.

*** Corresponding author.

E-mail addresses: yanxy@ibp.ac.cn (X. Yan), dmduan@ibp.ac.cn (D. Duan), gaolizeng@ibp.ac.cn (L. Gao).

¹ These authors contributed equally to this work.

<https://doi.org/10.1016/j.bios.2022.114739>

Received 16 July 2022; Received in revised form 12 September 2022; Accepted 15 September 2022

Available online 19 September 2022

0956-5663/© 2022 Elsevier B.V. All rights reserved.

testing times and requirements for biosafety laboratories and skilled technicians are not conducive for home testing or for use in remote rural areas, especially in low-income countries (Orach, 2009). To resolve this issue, a simple, rapid, inexpensive, and sensitive point-of-care testing (POCT) technology is critical for the diagnosis and prevention of COVID-19.

In contrast to RT-PCR, which requires precise temperature control, isothermal amplification has garnered increasing attention in recent decades as it offers an excellent opportunity to design rapid and portable molecular detection assays for use on-site. Isothermal amplification technologies include recombinase polymerase amplification (RPA), loop-mediated isothermal amplification, rolling circle amplification, cross-priming amplification, helicase-dependent amplification, and strand displacement amplification (Ma, 2022). Notably, RPA, which relies on recombinase, single-stranded DNA-binding protein, and strand-displacing DNA polymerase in the reaction, has shown considerable potential in the development of POCT for nucleic acid detection due to its high sensitivity, simple operation and primer design, rapid amplification, and low reaction temperatures (37–42 °C) (Magro et al., 2017; Piepenburg et al., 2006). Gold colloid-based lateral flow assays can convert RPA products into visual signals (Li et al., 2019). However, method sensitivity still needs to be improved to reach the level of RT-PCR (Patchsung et al., 2020; Tang et al., 2022).

We previously developed a lateral flow assay by replacing gold colloids with nanozymes (i.e., nanomaterial with enzyme-like activity) to amplify the detection signal and improve test-strip sensitivity (Gao et al., 2007). We successfully validated these nanozyme strips for Ebola (Duan et al., 2015) and SARS-CoV-2 antigen detection (Liu et al., 2021) by catalyzing the colorimetric (e.g., 3,3'-diaminobenzidine (DAB)) and chemiluminescent reactions (e.g., luminol). These nanozyme strips rapidly detect viral protein antigens through specific antibody recognition. As the nanozymes catalyze their substrate to amplify signals, the detection sensitivity of the nanozyme strips can be improved by 1–2 orders of magnitude compared to standard colloidal gold strips. In addition, compared to natural enzymes, nanozymes exhibit high stability, low cost, and tunable catalytic activity, making them ideal candidates for developing POCT. These studies encouraged us to expand the nanozyme strips for nucleic acid detection to meet the challenge of other viral infections such as COVID-19.

Here, we developed an RPA-conjugated FeS₂ nanozyme strip for rapid and sensitive nucleic acid detection of SARS-CoV-2, combining the rapid nucleic acid amplification function of RPA and signal-enhancing function of FeS₂ nanozymes with high peroxidase-like activity. Our assay detected nucleic acids of SARS-CoV-2 (RNA virus) at 200 copies/mL and human papilloma virus (HPV; DNA virus) at 500 copies/mL within 36 min, at sensitivities close to that of RT-PCR. Clinical samples were used for reliability and practicability validation. Using non-toxic 3,3',5,5'-tetramethylbenzidine (TMB) rather than carcinogenic DAB as the chromogenic substrate significantly amplified the strip signal, thus ensuring method safety. Our assay requires minimal training and simple equipment and is well suited for on-site detection due to its high sensitivity, short detection time, easy signal readout, and simple operation. Thus, these RPA-conjugated nanozyme strips show considerable potential as POCT candidates for convenient screening of infectious viruses such as SARS-CoV-2 and HPV.

2. Materials and methods

2.1. Reagents and materials

Polyvinyl pyrrolidone (PVP, MW: 10 000), FeCl₃, NaAc, NaAc·3H₂O, HCl, ethylene glycol, and streptavidin were purchased from Sigma-Aldrich Co. LLC. (Shanghai, China). Sulfur powder was obtained from Shanghai Aladdin Biochemical Technology Co., Ltd. (China). Both H₂O₂ and HAc were purchased from Sinopharm Chemical Reagent Co., Ltd. The DAB and 3-amino-9-ethylcarbazole (AEC) chromogenic kits were

purchased from Beijing Zhongshan Jinqiao Biotechnology Co., Ltd. (China). The ultrasensitive DAB chromogenic kit with enhancer was purchased from Sangon Biotech (Shanghai) Co., Ltd. (China). Precipitate-type TMB chromogenic substrate solution was purchased from Beijing Zoman Biotechnology Co., Ltd. (China). The fast nucleic acid releasing agent was obtained from Amp-Future (Changzhou) Biotech Co., Ltd. (China). The TwistAmp Basic kit was purchased from Beijing Libo Taiye Science and Technology Co., Ltd. (China) and MORUI (Shanghai) Biotechnology Co., Ltd. (China). The plasmids and primers were synthesized by Beijing Tsingke Biotechnology Co., Ltd. (China) and Suzhou Hongxun Biotechnologies Co., Ltd. (China). The sequences are presented in Tables S1–2. The nitrocellulose membrane was purchased from Sartorius (Germany). Fiberglass pads, absorbent pads, and polyvinylchloride (PVC) plastic boards were purchased from Shanghai Kinbio Tech. Co. Ltd. (China). Biotin was purchased from Thermo Scientific. The anti-digoxigenin antibodies were purchased from Xiamen Tongrenxin Biotechnology Co., Ltd. (China).

2.2. Synthesis of FeS₂ nanozymes

First, 0.1 g of PVP was dissolved in 30 mL of ethylene glycol, followed by the addition of 0.3 g of anhydrous FeCl₃. Then, 3.6 g of NaAc·3H₂O was added under constant magnetic stirring. Finally, 0.4 g of sulfur powder was added for ultrasonic dispersion, with the solution then poured into a 40-mL reactor for reaction at 200 °C for 12 h. After cooling to room temperature, the products were washed with ethanol three times and with water three times. The as-prepared nanozymes were then freeze-dried.

2.3. Characterization of FeS₂ nanozymes

Transmission electron microscopy (TEM), energy dispersive X-ray spectroscopy (EDS), and selected area electron diffraction (SAED) assays were performed using a FEI Tecnai G2 F30 TEM. Scanning electron microscopy (SEM) images were acquired using a S-4800II SEM (Hitachi, Japan). Dynamic light scattering and zeta potential were measured on a 90Plus PALS particle size and zeta potential analyzer. X-ray photoelectron spectroscopy (XPS) data were obtained using a 250Xi (Thermo Scientific, USA). X-ray diffraction (XRD) was performed using a D8 Advance (Bruker-AXS, Germany).

2.4. Peroxidase activity and kinetic assay of FeS₂ and Fe₃O₄ nanozymes

Peroxidase activity and kinetic assay of FeS₂ and Fe₃O₄ nanozymes were examined using standard assays (Jiang et al., 2018). The reaction buffer was 0.2 M NaAc-HAc buffer (pH 3.6) and the system contained 1 M H₂O₂, 2 mM TMB, and different amounts of nanozymes (0, 0.078125, 0.15625, 0.3125, and 0.625 μg). The reaction was carried out at 37 °C and detected using a U-3900 spectrophotometer (Hitachi, Japan). Specific activity was determined according to established standard methods. For the kinetic assay with H₂O₂ as the substrate, the reaction contained 25 μg/mL Fe₃O₄ or 10 μg/mL FeS₂ nanozymes, 2 mM TMB, and different concentrations of H₂O₂ (0, 0.05, 0.1, 0.2, 0.4, 0.6, 0.8, and 1 M for Fe₃O₄, and 0, 0.05, 0.1, 0.2, 0.4, 0.6, 0.8, and 1 mM for FeS₂). For the kinetic assay with TMB as the substrate, the reaction contained 25 μg/mL Fe₃O₄ or 0.1 μg/mL FeS₂ nanozymes, 1 M H₂O₂, and different concentrations of TMB (0, 0.1, 0.2, 0.4, 0.8, 1.2, 1.6, and 2 mM for Fe₃O₄, and 0, 1.6, 2.4, 3.2, 4, 4.8, and 6.4 mM for FeS₂). The kinetic parameters were calculated according to established standards.

2.5. Preparation of FeS₂ nanozyme probes

Preparation of the FeS₂ nanozyme probes was performed following the preparation method of colloidal gold probes (Shyu et al., 2002). First, the pH of 200 μg/mL FeS₂ nanozyme aqueous solution was adjusted with K₂CO₃ to 0.5 higher than the isoelectric point of

streptavidin, i.e., pH 6.5. Different amounts of streptavidin (0, 5, 10, 20, and 40 μg) were added and the mixture was rotated at room temperature for 10 min. The FeS_2 nanozyme probes were then blocked by 1% (w/v) bovine serum albumin (BSA) at room temperature for 10 min and centrifuged at 7000 rpm for 5 min. The nanozyme probes were finally resuspended in 20 mM Tris/HCl buffer (pH 8.2) containing 1% BSA.

2.6. Preparation of FeS_2 nanozyme-strip

The nanozyme strip consists of a PVC plastic board, an absorbent pad, a sample pad, and a nitrocellulose membrane. Fabrication of the FeS_2 nanozyme strips followed our previous study (Duan et al., 2015). First, a nitrocellulose membrane was attached to a PVC plastic board, with the test line and control line then dispensed (0.1 μL per 1 mm line) along the nitrocellulose membrane sheet using an IsoFlow™ Dispenser (Imagene Technology, New Hampshire, USA). Biotin was first combined with BSA to better bind to the nitrocellulose membrane, and then was sprayed to the control line at a concentration of 1 mg/mL. Anti-digoxigenin antibody was sprayed on the test line at a concentration of 3 mg/mL. The nitrocellulose membrane was dried at 37 °C for 1 h, blocked with 1% BSA for 30 min, washed three times (5 mM borate buffer, pH 8.8), then dried again at 37 °C for 3 h. The absorbent pads were glued to the PVC plastic board overlapping the nitrocellulose membrane. The nitrocellulose membrane sheets were then cut into test strips (25 mm \times 5 mm) using a microtome (Economic Cutter ZQ2000, Shanghai Kinbio Tech Co. Ltd., Shanghai, China). The prepared strips were placed in a sealed bag and stored in a dry place at room temperature.

2.7. FeS_2 nanozyme-strip test for nucleic acid detection of SARS-CoV-2

Synthetic viral template was amplified by RPA according to the manufacturer's instructions, with some modification to obtain a large number of target products. Briefly, the 50- μL reaction contained 2.4 μL of forward primer (6.7 μM), 2.4 μL of reverse primer (6.7 μM), 29.5 μL of primer free rehydration buffer, and 13.2 μL of SARS-CoV-2 template at different concentrations. After shaking and mixing, the reaction mixture was added to a TwistAmp Basic reaction and mixed by pipetting. Finally, 2.5 μL of 280 mM magnesium acetate was added, mixed well, and reacted at 39 °C for 20 min. At 4 min, the reaction system was shaken, mixed, and centrifuged briefly. The target products were diluted with 20 mM Tris-HCl (pH 8.0), after which 100 μL of target product was mixed with the FeS_2 nanozyme probes and dropped onto the sample pad on the strip. After 10 min of chromatography, the strip was transferred to the prepared mixed solution containing precipitate-type TMB and H_2O_2 for 6 min, with the reaction terminated using deionized water. Finally, an immunoquantitative analyzer was used to analyze the test results of the strip.

2.8. FeS_2 nanozyme-strip test for nucleic acid detection of HPV-16

Cervical secretions from 14 HPV-16-positive patients and 14 healthy individuals were collected from the Xishan People's Hospital, Wuxi City, Jiangsu Province, China. This study was conducted in accordance with all ethical standards and was approved by the corresponding ethics committee. Before sample collection, informed consent was obtained from all participants. Nucleic acid was extracted from the clinical virus samples using a fast nucleic acid releasing agent according to the manufacturer's instructions. Extracted nucleic acids and synthetic template of HPV-16 were amplified by RPA and then detected using the FeS_2 nanozyme strip following the same procedures as the detection of SARS-CoV-2.

2.9. Statistical analysis

All data are presented as mean \pm standard deviation ($n = 3$) and

analyzed using GraphPad Prism v8.0.2. Error bars shown represent standard error derived from three independent measurements.

3. Results and discussion

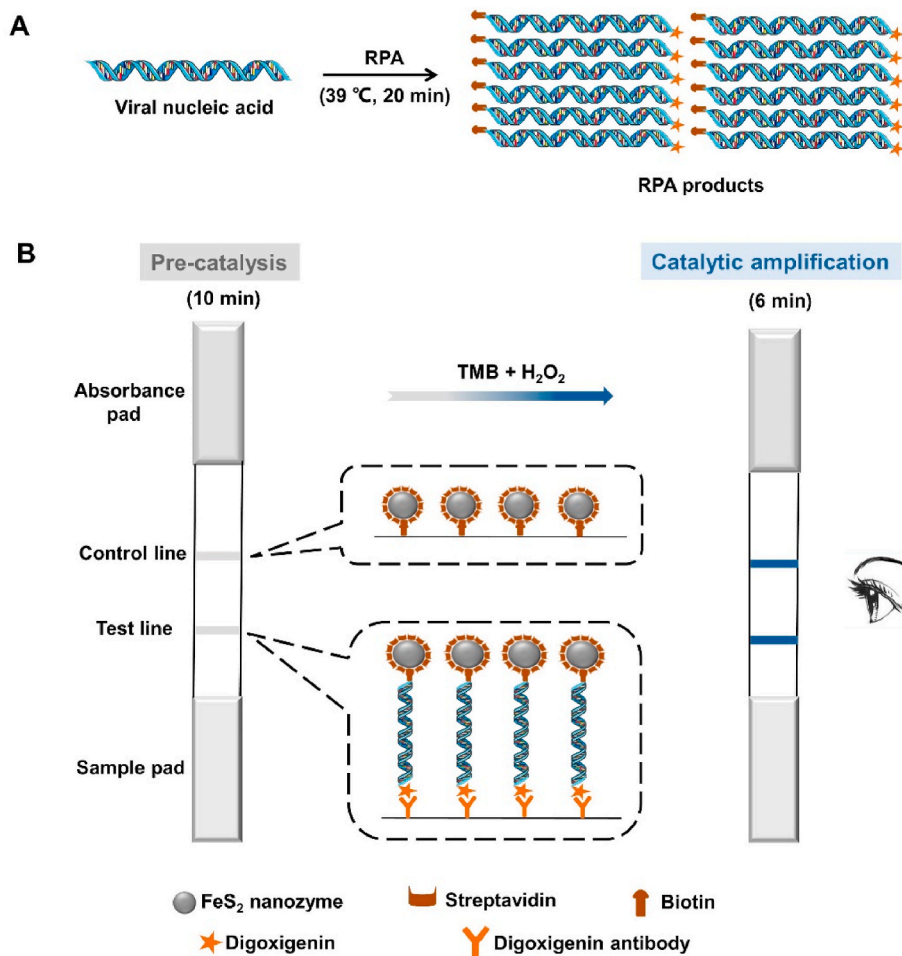
3.1. Principles of nanozyme strip for nucleic acid detection

The process of nucleic acid detection using the FeS_2 nanozyme strips is shown in Scheme 1, and consists of RPA amplification, strip chromatography, and catalytic amplification. Firstly, the nucleic acids are amplified by RPA (Fig. S1), completed at 39 °C for 20 min. The forward and reverse primers contain biotin and digoxin markers, respectively, thus allowing RPA products containing biotin-digoxin double markers to be obtained. The strip consists of an absorbent pad, a nitrocellulose membrane containing control and test lines, and a sample pad. The control line is sprayed with the BSA-biotin complex, and the test line is sprayed with the anti-digoxigenin antibodies. The FeS_2 nanozymes are modified by streptavidin to form nanozyme probes. In the presence of nucleic acid amplification products, the FeS_2 nanozyme probes react with biotin at one end of the products, and then migrate to the absorbent pad through capillary action. When the sample reaches the test line, the digoxigenin at the other end of the products binds to the digoxigenin antibodies. At high concentrations of nucleic acid, this line is visible due to the color of the FeS_2 nanozymes. The excess nanozyme probes continue to migrate to the control line and are captured by the coated BSA-biotin. In the absence of nucleic acid targets, the FeS_2 nanozyme probes directly bind to the control line biotin. After 10 min of chromatography, the test strip is immersed in a mixed solution containing precipitate-type TMB and H_2O_2 . The peroxidase-like activity of the FeS_2 nanozymes catalyzes the production of insoluble oxidized TMB products, resulting in the amplification of signals and detection of trace nucleic acid-amplified products, thereby improving detection sensitivity. After 6 min, the detection results can be interpreted with the naked eye, with two lines (control line and test line) indicating a positive case and one line (control line) representing a negative case. The total procedure, including amplification and strip testing, can be completed within 36 min.

3.2. Synthesis and characterization of FeS_2 nanozymes

The FeS_2 nanozymes were synthesized by adding a source of S during a one-pot solvothermal reaction with iron salts (Meng et al., 2021). PVP was introduced as a surfactant to increase dispersibility and stability. The TEM (Fig. 1A) and SEM images (Fig. S2A) showed that the as-prepared nanozymes were uniform particles in size with a diameter of about 255 nm (Fig. S2B). The nanozymes were well-dispersed in water, with a mean hydrodynamic diameter of 278 nm (Fig. S3). Elemental analysis by XPS indicated that the prepared nanozymes mainly consisted of Fe and S, and the C, N, and O signals confirmed the presence of the PVP surfactant (Fig. S4A). The valence states of Fe and S were further assessed, as shown in Figs. S4B–C and Tables S3–4. The Fe 2p peaks at 707.17 (2p_{3/2}) and 719.79 eV (2p_{1/2}) were assigned to Fe^{2+} , and the S 2p peaks at 162.53 (2p_{3/2}) and 163.73 eV (2p_{1/2}) were ascribed to S_2^{2-} . The weak peaks attributed to Fe^{3+} and S–O were caused by surface oxidation, a common phenomenon for Fe^{2+} and S_2^{2-} (Tang et al., 2017). EDS elemental mapping demonstrated homogeneous distributions of Fe, S, C, N, and O over the whole nanoparticle (Fig. S4D). XRD was employed to study the crystal structure of the obtained nanozymes. Results showed that all sharp and well-defined diffraction peaks were readily indexed to the pure cubic phase of pyrite FeS_2 (PDF 71–0053; Fig. 1B). SAED analysis showed polycrystalline rings, indicating that the FeS_2 nanozymes were polycrystalline structures (Fig. 1C).

We also investigated the peroxidase-like activity of the FeS_2 nanozymes. In the presence of the nanozymes and H_2O_2 , TMB was oxidized with characteristic absorption peaks at 370 nm and 652 nm, thus confirming the peroxidase-like activity of the FeS_2 nanozymes (Fig. 1D).



Scheme 1. Illustration of nanozyme strip combined with RPA for nucleic acid detection.

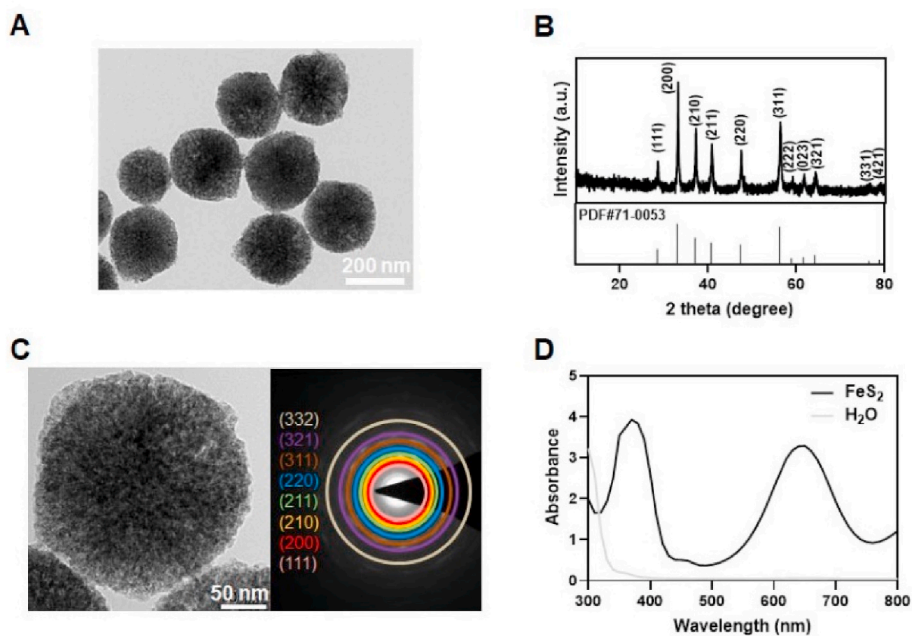


Fig. 1. Synthesis and characterization of FeS₂ nanozymes. (A) TEM image of FeS₂ nanozymes. (B) XRD pattern of FeS₂ nanozymes. (C) SAED pattern of FeS₂ nanozymes. (D) Ultraviolet-visible absorbance spectra of oxidized TMB after catalysis of FeS₂ nanozymes.

Furthermore, the enzymatic activity was nanozyme mass-dependent (Fig. S5A), with specific activity of 47.98 U mg^{-1} (Fig. S5B). In contrast, a previous study reported a specific activity value of 1.958 U mg^{-1} for similarly sized and synthesized Fe_3O_4 nanozymes (Jiang et al., 2018). Therefore, the peroxidase-like activity of the FeS_2 nanozymes was 24.5 times higher than that of the Fe_3O_4 nanozymes, which is beneficial for the amplification of the colorimetric signal on the test strip. To understand the mechanism for the higher peroxidase-like activity, we performed enzyme kinetic analysis of the two nanozymes (Figs. S5C–F and Table S5). Results showed that the FeS_2 nanozymes had higher affinity for H_2O_2 and higher catalytic ability for both H_2O_2 and TMB than the Fe_3O_4 nanozymes, which contributed to their high peroxidase-like activity.

3.3. Preparation of FeS_2 nanozyme probes

The FeS_2 nanozyme probes were prepared by modification of streptavidin on the surface of the nanozymes to capture biotin-labeled RPA products. Streptavidin modification resulted in a slight increase in the hydrodynamic diameter (Fig. S6A) and zeta potential (Fig. S6B) of the FeS_2 nanozymes. By optimizing the amount of streptavidin in the modification system, we found that modification of $20 \mu\text{g}$ of streptavidin with $200 \mu\text{g}$ of FeS_2 nanozymes reached saturation. The TEM images (Fig. S6C) showed that the FeS_2 nanozymes had a clear, gray protein corona on their surface, confirming successful streptavidin modification on the nanozymes.

3.4. Construction and optimization of FeS_2 nanozyme strips

Optimization of the FeS_2 nanozyme strips for nucleic acid detection included the chromogenic substrate, H_2O_2 substrate dosage for nanozyme catalysis, catalytic time, and FeS_2 nanozyme probe amount, which can all affect the ability of the nanozymes to enhance the colorimetric signals. Typical peroxidase chromogenic substrates, i.e., DAB (with enhancer), TMB, and AEC, were tested due to their ability to be catalyzed to produce insoluble precipitates. As shown in Fig. 2A, when TMB was used as the chromogenic substrate, the test strip generated the most obvious signals after nanozyme catalysis compared to that before catalysis. Therefore, we chose TMB as the chromogenic substrate for the FeS_2 nanozyme strips. Of note, TMB is the only nontoxic substance among these substrates, which is beneficial for the safety of

experimenters and future product transformation. We next optimized the H_2O_2 substrate dosage and catalytic time and found that $80 \mu\text{L}$ of H_2O_2 (30%) (Fig. 2B) and 6 min (Fig. 2C) of catalysis achieved the best catalytic enhancement effect on the FeS_2 nanozyme strips. We then optimized the FeS_2 nanozyme probe amount. Because excess nanozyme probes combine with the control line biotin, the control line color gradually deepened with the increase in nanozyme probes. Therefore, we quantified the control line of the test strip and found that $2 \mu\text{g}$ of FeS_2 nanozyme probes achieved the best enhancement effect and reached colorimetric signal saturation (Fig. 2D and Fig. S7).

3.5. FeS_2 nanozyme strip test for nucleic acid of SARS-CoV-2

A 172-nucleotide segment within the ORF1ab gene of SARS-CoV-2 from the NCBI Reference sequence (NC-045512.2) was chosen as the detection target. This segment is reported to be conserved in the wide-type virus and most mutated strains (Tang et al., 2022). The target sequence and forward and reverse RPA primers are shown in Fig. 3A. To determine the detection sensitivity of the FeS_2 nanozyme strips for SARS-CoV-2, synthetic templates at different concentrations were introduced for RPA amplification, with the RPA products then detected using the strip. Results showed that a limit of detection (LOD) of 1000 copies/mL was achieved without signal amplification (Fig. 3B left). Importantly, after FeS_2 nanozyme catalysis, the LOD reached 200 copies/mL (Fig. 3B right). This LOD is lower than that of other visual nucleic acid detection methods for SARS-CoV-2 and is also simpler and less time-consuming (Table 1).

To compare the FeS_2 nanozyme strips with other current nucleic acid detection methods, we replaced the nanozyme probes with colloidal gold probes. Results showed that the LOD of the colloidal gold strips was 1000 copies/mL, the same as that of the FeS_2 nanozyme strips without the catalytic procedure (Fig. 3C). This result suggests that enzymatic enhancement of the FeS_2 nanozyme strips is required for higher sensitivity. To verify the detection specificity of the FeS_2 nanozyme strips, genes from several other RNA viruses, including Middle East respiratory syndrome coronavirus (MERS-CoV), Ebola, and Zika, were used for RPA. As seen in Fig. 3D, the nanozyme strips only detected the SARS-CoV-2 template, not the templates of other viruses, thus confirming the high specificity of the RPA reaction and FeS_2 nanozyme strips.

It is important to note that due to the conservation of the sequence selected, this method can detect both wild-type and mutant viruses of

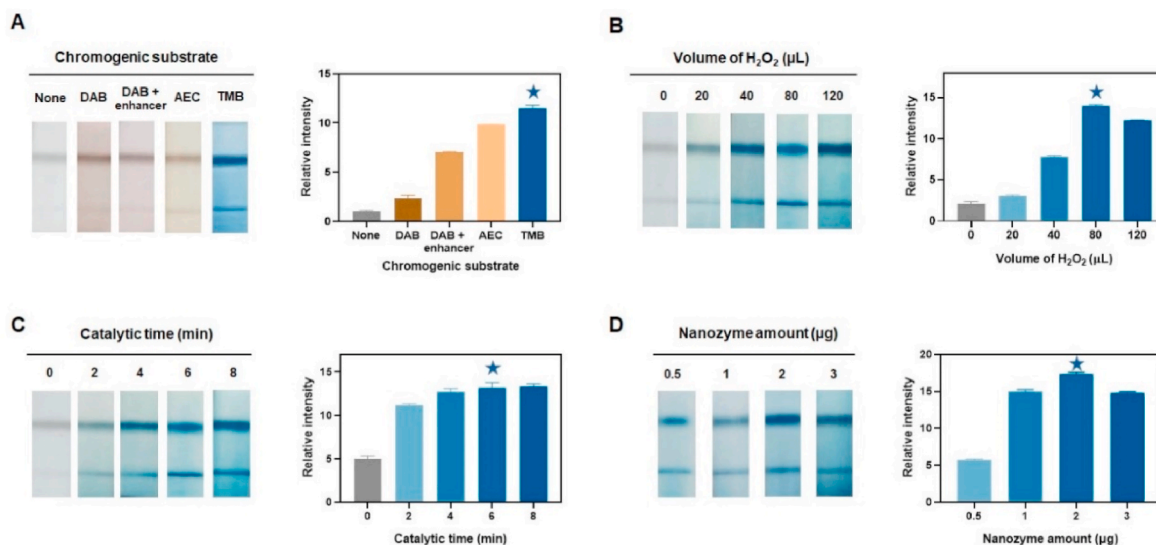


Fig. 2. Construction and optimization of nanozyme strips. (A) Strips and relative intensity of test line with different chromogenic substrates. (B) Strips and relative intensity of test line with different volumes of H_2O_2 substrate. (C) Strips and relative intensity of test line with different catalytic time. (D) Strips and relative intensity of control line with different amounts of FeS_2 nanozyme after catalysis.

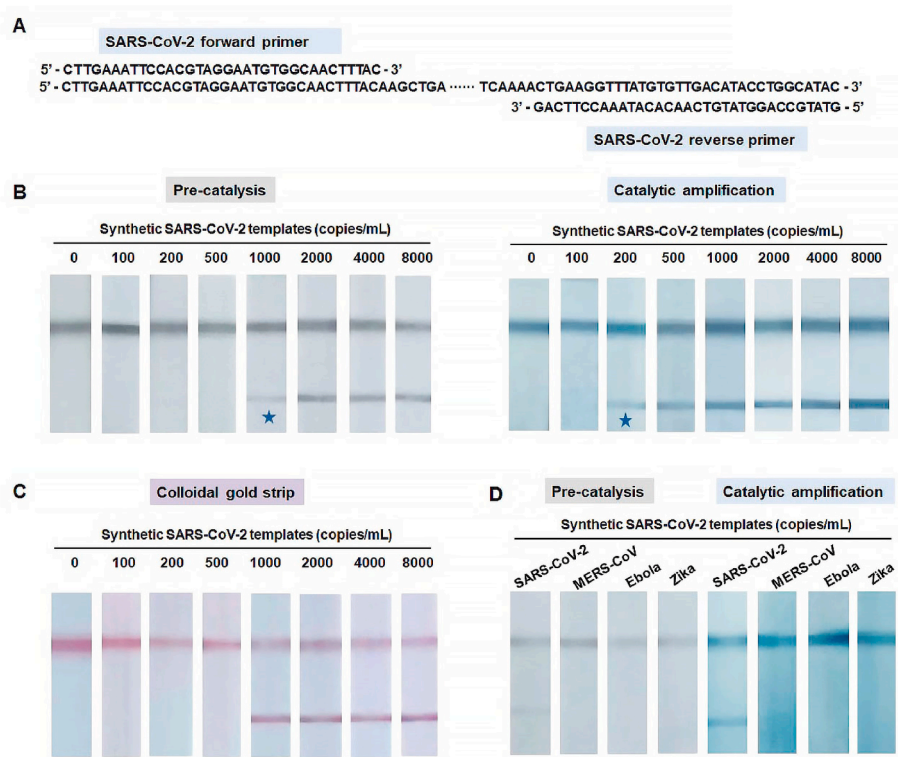


Fig. 3. Fe₂S₂ nanozyme strip for nucleic acid detection of SARS-CoV-2. (A) Sequence and RPA primers of SARS-CoV-2 (within ORF1ab gene) under detection. (B) Fe₂S₂ nanozyme strip for detection of different concentrations of synthetic SARS-CoV-2 templates before (left) and after (right) catalytic amplification. (C) Colloidal gold strip for detection of different concentrations of synthetic SARS-CoV-2 templates. (D) Fe₂S₂ nanozyme strip for nucleic acid detection of other RNA viruses.

Table 1

Comparison of different visual detection methods for nucleic acids of SARS-CoV-2.

Method	LOD (copies/mL)	Time (min)	Reference
CRISPR–Cas12-based detection	10 000	32–42	Broughton et al. (2020)
SHERLOCK One-Pot Testing	33	80	Joung et al. (2020)
Two-Step SHERLOCK detection	6462	70	Patchsung et al. (2020)
CLIPON	2000	90	Tang et al. (2022)
CHA-LFIA detection	2000	33	Zou et al. (2021)
RT-PCR	580	180	Corman et al. (2020)
Fe ₂ S ₂ nanozyme-strip	200	36	This work

SARS-CoV-2. Clarification of different mutants can be detected by designing corresponding primers for RPA.

3.6. Fe₂S₂ nanozyme-strip test for nucleic acids of HPV-16 and clinical samples

As a high-risk HPV, HPV-16 is responsible for more than 50% of cervical cancers (Hwang et al., 2016). Here, HPV-16 (DNA virus) was chosen to verify the versatility of nucleic acid detection using the Fe₂S₂ nanozyme strips. The target sequence and forward and reverse RPA primers of HPV-16 are presented in Fig. 4A. As seen in Fig. 4B, the LOD was 2000 copies/mL before catalysis but 500 copies/mL after catalysis amplification. This not only confirmed that Fe₂S₂ nanozyme catalysis improved the detection sensitivity of the strip, but also that these highly sensitive strips could be used for the detection of other viruses. In contrast, the LOD of the colloidal gold strips for nucleic acid detection of HPV-16 was higher (2000 copies/mL) than that of the Fe₂S₂ nanozyme strip (Fig. S8).

Clinical samples of HPV-16 were tested to further confirm the reliability and practicability of the Fe₂S₂ nanozyme strips (Fig. 4C). These clinical samples were previously tested by RT-PCR, with ct values greater than 36 representing a negative result, otherwise representing a positive result. DNA of the HPV-16 samples was extracted using a kit and facile procedure. Using the Fe₂S₂ nanozyme strips, we obtained 14 positive clinical samples (Fig. 4D and Fig. S9) and 14 negative clinical samples (Fig. 4E and Fig. S10), which were 100% consistent with the RT-PCR results, with no false positives or false negatives. Thus, the Fe₂S₂ nanozyme strips for nucleic acid detection exhibit good application potential for viral infections.

4. Conclusions

We developed a novel method for rapid and sensitive nucleic acid detection of viruses by combining RPA with a nanozyme strip. Given their high peroxidase-like activity, the Fe₂S₂ nanozyme strips utilized nontoxic TMB as a substrate to amplify the colorimetric signal. Our system achieved a LOD close to that of typical RT-PCR for SARS-CoV-2 and HPV-16. Therefore, the combined strategy can extend the application of nanozyme strips from protein detection to nucleic acid detection with high sensitivity to SARS-CoV-2 and other viruses. Of noted, the specificity of such system mainly depends on RPA, therefore, the primers for RPA need to be carefully designed to prevent primer-dimers formation which may cause false-positive result. In addition, to achieve practicable POCT with high specificity and sensitivity, integrated device that can automatically conduct sample processing, RPA and nanozyme-strip assay needs to be considered.

CRediT authorship contribution statement

Xiangqin Meng: Investigation, Formal analysis, Writing – original draft. **Sijia Zou:** Investigation, Formal analysis, Writing – original draft.

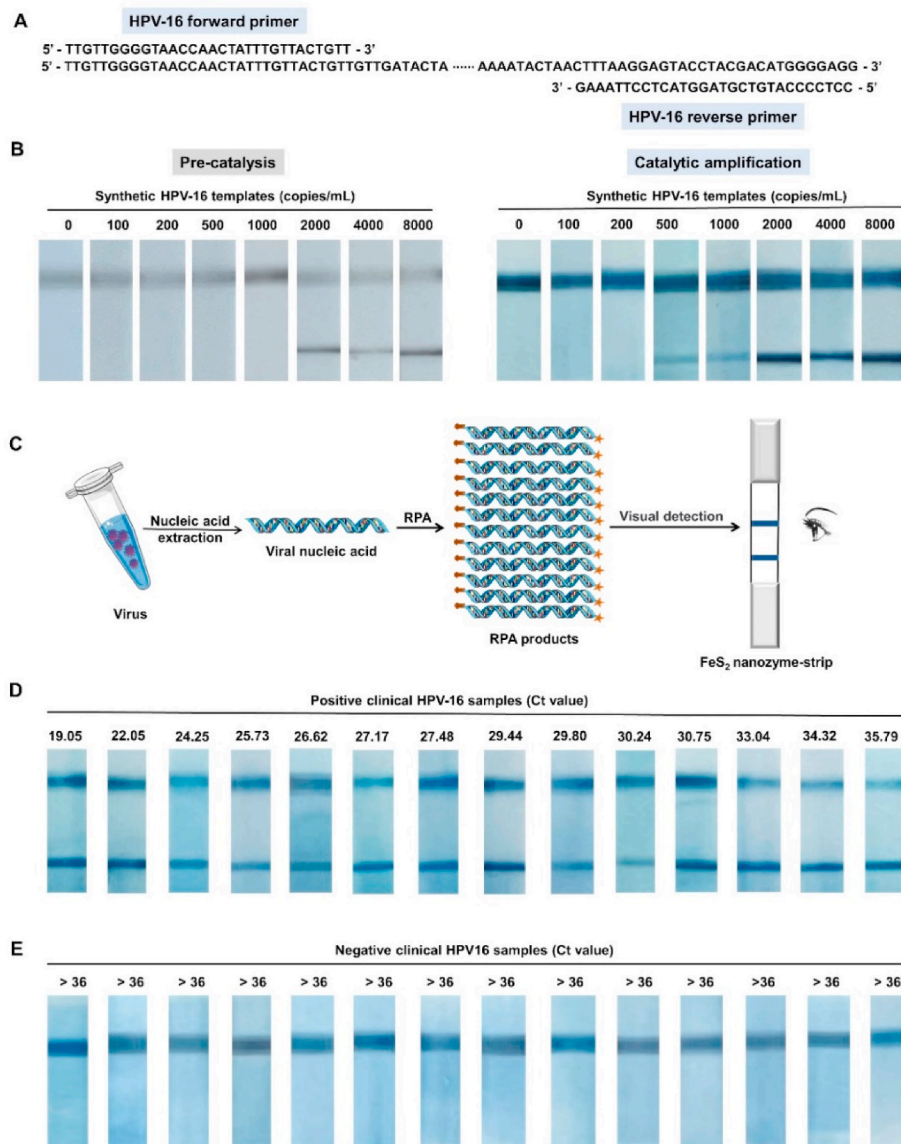


Fig. 4. Fe₂ nanozyme strip for nucleic acid detection of HPV-16. (A) Sequence and RPA primers of HPV-16 under detection. (B) Fe₂ nanozyme strip for detection of different concentrations of HPV-16 synthetic templates before (left) and after (right) catalytic amplification. (C) Fe₂ nanozyme strip for nucleic acid detection of HPV-16 clinical samples. (D) Fe₂ nanozyme strip for detection of positive clinical HPV-16 samples after catalytic amplification. (E) Fe₂ nanozyme strip for detection of negative clinical HPV-16 samples after catalytic amplification.

Dandan Li: Resources, Methodology. **Jiuyang He:** Writing – review & editing, Validation. **Ling Fang:** Resources. **Haojue Wang:** Resources. **Xiyun Yan:** Conceptualization, Writing – review & editing, Supervision, Funding acquisition. **Demin Duan:** Conceptualization, Writing – review & editing, Supervision, Funding acquisition. **Lizeng Gao:** Conceptualization, Writing – review & editing, Supervision, Funding acquisition.

Declaration of competing interest

The authors declare that they have no known competing financial interests or personal relationships that could have appeared to influence the work reported in this paper.

Data availability

Data will be made available on request.

Acknowledgments

This work was supported by the National Key R&D Program of China grant 2019YFA0709200 (L.G.), as well as the National Natural Science

Foundation of China Grant 82072324 (D.D.), 81930050 (X.Y.), National Natural Science Foundation of China of Innovative Research Group grant 22121003 (X.Y. and L.G.), Wuxi Science and Technology Plan Project N2020 × 018 (H.W.), the scientific research project plan of Wuxi Municipal Health Commission was approved and funded M202007 (H.W.), The Top Talent Support Program for young and middle-aged people of Wuxi Health Committee bj2020111 (H.W.).

Appendix A. Supplementary data

Supplementary data to this article can be found online at <https://doi.org/10.1016/j.bios.2022.114739>.

References

- Broughton, J.P., Deng, X.D., Yu, G.X., Fasching, C.L., Servellita, V., Singh, J., Miao, X., Streithorst, J.A., Granados, A., Sotomayor-Gonzalez, A., Zorn, K., Gopez, A., Hsu, E., Gu, W., Miller, S., Pan, C.Y., Guevara, H., Wadford, D.A., Chen, J.S., Chiu, C.Y., 2020. Nat. Biotechnol. 38, 870–874.
- Corman, V.M., Landt, O., Kaiser, M., Molenkamp, R., Meijer, A., Chu, D.K., Bleicker, T., Brunink, S., Schneider, J., Schmidt, M.L., Mulders, D.G., Haagmans, B.L., van der Veer, B., van den Brink, S., Wijsman, L., Goderski, G., Romette, J.L., Ellis, J., Zambon, M., Peiris, M., Goossens, H., Reusken, C., Koopmans, M.P., Drosten, C., 2020. Euro Surveill. 25, 2000045.

- Duan, D.M., Fan, K.L., Zhang, D.X., Tan, S., Liang, M.F., Liu, Y., Zhang, J.L., Zhang, P.H., Liu, W., Qiu, X.G., Kobinger, G.P., Gao, G.F., Yan, X.Y., 2015. *Biosens. Bioelectron.* 74, 134–141.
- Gao, L.Z., Zhuang, J., Nie, L., Zhang, J.B., Zhang, Y., Gu, N., Wang, T.H., Feng, J., Yang, D.L., Perrett, S., Yan, X.Y., 2007. *Nat. Biotechnol.* 2, 577–583.
- Hwang, S.H., Kim, D.E., Im, J.H., Kang, S.J., Lee, D.H., Son, S.J., 2016. *Biosens. Bioelectron.* 79, 829–834.
- Iketani, S., Liu, L.H., Guo, Y.C., Liu, L.Y., Chan, J.F.W., Huang, Y.M., Wang, M., Luo, Y., Yu, J., Chu, H., Chik, K.K.H., Yuent, T.T.T., Yin, M.T., Sobieszczyk, M.E., Huang, Y. X., Yuen, K.Y., Wang, H.H., Sheng, Z.Z., Ho, D.D., 2022. *Nature* 604, 553–556.
- Jiang, B., Duan, D.M., Gao, L.Z., Zhou, M.J., Fan, K.L., Tang, Y., Xi, J.Q., Bi, Y.H., Tong, Z., Gao, G.F., Xie, N., Tang, A.F., Nie, G.H., Liang, M.M., Yan, X.Y., 2018. *Nat. Protoc.* 13, 1506–1520.
- Joung, J., Ladha, A., Saito, M., Kim, N.G., Woolley, A.E., Segel, M., Barretto, R.P.J., Ranu, A., Macrae, R.K., Faure, G., Ioannidi, E.I., Krajeski, R.N., Bruneau, R., Huang, M.W., Yu, X.G., Li, J.Z., Walker, B.D., Hung, D.T., Greninger, A.L., Jerome, K. R., Gootenberg, J.S., Abudayyeh, O.O., Zhang, F., 2020. *N. Engl. J. Med.* 383, 1492–1494.
- Li, J., Macdonald, J., von Stetten, F., 2019. *Analyst* 144, 31–67.
- Li, Q.Q., Wu, J.J., Nie, J.H., Zhang, L., Hao, H., Liu, S., Zhao, C.Y., Zhang, Q., Liu, H., Nie, L.L., Qin, H.Y., Wang, M., Lu, Q., Li, X.Y., Sun, Q.Y., Liu, J.K., Zhang, L.Q., Li, X. G., Huang, W.J., Wang, Y.C., 2020. *Cell* 182, 1284–1294.
- Liu, D., Ju, C.H., Han, C., Shi, R., Chen, X.H., Duan, D.M., Yan, J.H., Yan, X.Y., 2021. *Biosens. Bioelectron.* 173, 112817.
- Ma, X.J., 2022. *Zoon* 2, 1.
- Magro, L., Jacquelin, B., Escadafal, C., Garneret, P., Kwasiborski, A., Manuguerra, J.C., Monti, F., Sakuntabhai, A., Vanhomwegen, J., Lafaye, P., Tabeling, P., 2017. *Sci. Rep.* 7, 1347.
- Meng, X.Q., Li, D.D., Chen, L., He, H.L., Wang, Q., Hong, C.Y., He, J.Y., Gao, X.F., Yang, Y.L., Jiang, B., Nie, G.H., Yan, X.Y., Gao, L.Z., Fan, K.L., 2021. *ACS Nano* 15, 5735–5751.
- Orach, C.G., 2009. *Afr. Health Sci.* 9, 549–551.
- Patchsung, M., Jantarug, K., Pattama, A., Aphicho, K., Suraritdechachai, S., Meesawat, P., Sappakhaw, K., Leelahakorn, N., Ruenkam, T., Wongsatit, T., Athipanyasilp, N., Eiamthong, B., Lakkansirorat, B., Phoodokmai, T., Niljianskul, N., Pakotiprapha, D., Chanarat, S., Homchan, A., Tinikul, R., Kamutira, P., Phiwkaow, K., Soithongcharoen, S., Kantiwiriyanitch, C., Pongsupasa, V., Trisrivirat, D., Jaroensuk, J., Wongnate, T., Maenpuen, S., Chaiyen, P., Kamnerdnakta, S., Swangsri, J., Chuthapisith, S., Sirivatanauksorn, Y., Chaimayo, C., Sutthent, R., Kantakamalakul, W., Joung, J., Ladha, A., Jin, X., Gootenberg, J.S., Abudayyeh, O.O., Zhang, F., Horthongkham, N., Uttamapinant, C., 2020. *Nat. Biomed. Eng.* 4, 1140–1149.
- Piepenburg, O., Williams, C.H., Stemple, D.L., Armes, N.A., 2006. *PLoS Biol.* 4, 1115–1121.
- Shih, H.I., Wu, C.J., Tu, Y.F., Chi, C.Y., 2020. *Biomed. J.* 43, 341–354.
- Shyu, R.H., Shyu, H.F., Liu, H.W., Tang, S.S., 2002. *Toxicol.* 40, 255–258.
- Tang, Z.M., Zhang, H.L., Liu, Y.Y., Ni, D.L., Zhang, H., Zhang, J.W., Yao, Z.W., He, M.Y., Shi, J.L., Bu, W.B., 2017. *Adv. Mater.* 29, 1701683.
- Tang, Y.D., Qi, L.J., Liu, Y.C., Guo, L.L., Zhao, R.J., Yang, M.T., Du, Y., Li, B.L., 2022. *Angew. Chem., Int. Ed. Engl.* 61, e202115907.
- Wang, C., Horby, P.W., Hayden, F.G., Gao, G.F., 2020. *Lancet* 395, 496, 496.
- Zou, M.Y., Su, F.Y., Zhang, R., Jiang, X.L., Xiao, H., Yan, X.J., Yang, C.K., Fan, X.B., Wu, G.Q., 2021. *Sensor. Actuator. B Chem.* 342, 129899.